Physics Letters B 843 (2023) 137995

Contents lists available at ScienceDirect

Physics Letters B

journal homepage: www.elsevier.com/locate/physletb

Next-to-leading-order QCD corrections to Higgs production in association with a jet

Roberto Bonciani [a], Vittorio Del Duca [b,c,d], Hjalte Frellesvig [e], Martijn Hidding [f], Valentin Hirschi [g], Francesco Moriello [h], Giulio Salvatori [i], Gábor Somogyi [j], Francesco Tramontano [k,*]

[a] Dipartimento di Fisica, Università di Roma "La Sapienza" and INFN Sezione di Roma, Piazzale Aldo Moro 2, 00185 Roma, Italy
[b] ETH Zürich, Institut für theoretische Physik, 8093 Zürich, Switzerland
[c] Physik-Institut, Universität Zürich, 8057 Zürich, Switzerland
[d] INFN, Laboratori Nazionali di Frascati, 00044 Frascati RM, Italy
[e] Niels Bohr International Academy, University of Copenhagen, Blegdamsvej 17, 2100 Copenhagen, Denmark
[f] Department of Physics and Astronomy, Uppsala University, SE-75120 Uppsala, Sweden
[g] Theoretical Physics Department, CERN, CH-1211 Geneva 23, Switzerland
[h] DSM AG, Wurmisweg 576, CH-4303 Kaiseraugst, Switzerland
[i] School of Natural Sciences, Institute for Advanced Study, Princeton, NJ, 08540, USA
[j] Wigner Research Centre for Physics, Konkoly-Thege Miklós u. 29-33, 1121 Budapest, Hungary
[k] Università di Napoli and INFN, Sezione di Napoli, Complesso Universitario di Monte Sant'Angelo, Via Cintia, 80126 Napoli, Italy

ARTICLE INFO

Article history:
Received 22 March 2023
Received in revised form 25 May 2023
Accepted 2 June 2023
Available online 12 June 2023
Editor: G.F. Giudice

ABSTRACT

We compute the next-to-leading-order (NLO) QCD corrections to the Higgs p_T distribution in Higgs production in association with a jet via gluon fusion at the LHC, with exact dependence on the mass of the quark circulating in the heavy-quark loops. The NLO corrections are presented including the top-quark mass, and for the first time, the bottom-quark mass as well. Further, besides the on-shell mass scheme, we consider for the first time a running mass renormalisation scheme. The computation is based on amplitudes which are valid for arbitrary heavy-quark masses.

© 2023 The Author(s). Published by Elsevier B.V. This is an open access article under the CC BY license (http://creativecommons.org/licenses/by/4.0/). Funded by SCOAP[3].

1. Introduction

Since the discovery of the Higgs boson [1,2], one of the main goals of the Large Hadron Collider (LHC) physics program has been to investigate its couplings and quantum numbers as accurately as possible. At the LHC, the dominant Higgs production mode is via gluon fusion, with the coupling of the Higgs boson to gluons being mediated by a heavy-quark loop. This gives the opportunity to test the Standard Model (SM) and to look for possible deviations from it, which would be footprints of New Physics (NP) [3–19].

The Higgs production cross section has been computed at leading order [20] and at next-to-leading-order (NLO) in strong coupling constant α_s for arbitrary quark masses in the heavy-quark loop [21,22], and at next-to-next-to-leading-order (NNLO) for the top-quark mass [23]. The exact calculation [23] lies within 1% of the result obtained at NNLO [24–26] in the Higgs Effective Field Theory (HEFT) approximation, i.e. in the limit of a top quark much heavier than the Higgs boson, $M_{\text{top}} \gg M_H$, with all other quarks taken as massless.

The chances of discriminating between the loop-mediated coupling of the full theory and the tree-level coupling of the HEFT, and thus of probing possible NP effects, are expected to rise in the phase space regions where the contribution of the hard gluons becomes relevant. In that respect, a promising observable is the Higgs p_T distribution [27–31], which allows one to analyse how the production rate depends on the heavy-quark loop at different p_T values. The Higgs p_T distribution is known at leading order in α_s for arbitrary quark masses in the heavy-quark loop [32–34], and at NLO for the top-quark mass [35,36] in the on-shell (OS) mass scheme. Approximate results are known at NLO [37], which include the bottom-quark mass [38–40] as well as the top-bottom interference [41], and beyond NLO in the high-energy limit [42]. Further, the mixed QCD-electroweak contributions to the Higgs p_T distribution are known at leading order [43]. The HEFT approach

* Corresponding author.
E-mail addresses: roberto.bonciani@roma1.infn.it (R. Bonciani), delducav@itp.phys.ethz.ch (V. Del Duca), hjalte.frellesvig@nbi.ku.dk (H. Frellesvig), martijn.hidding@physics.uu.se (M. Hidding), valentin.hirschi@cern.ch (V. Hirschi), francescomoriello@gmail.com (F. Moriello), giulio.salvatori.0@gmail.com (G. Salvatori), somogyi.gabor@wigner.hu (G. Somogyi), francesco.tramontano@unina.it (F. Tramontano).

https://doi.org/10.1016/j.physletb.2023.137995
0370-2693/© 2023 The Author(s). Published by Elsevier B.V. This is an open access article under the CC BY license (http://creativecommons.org/licenses/by/4.0/). Funded by SCOAP[3].

provides a good approximation to the Higgs p_T distribution when $p_T < m_t$ [33]. In HEFT, the Higgs p_T distribution is known at NNLO in α_s [44–47]. Conversely, when $p_T > m_t$ the shape of the Higgs p_T distribution in HEFT overshoots the exact Higgs p_T distribution [36].

In this letter, we present the Higgs p_T distribution at NLO in α_s, with top-quark mass dependence, and for the first time including also the exact bottom-quark mass contribution. Further, since the top- and bottom-quark masses are treated as dynamical parameters and not as fixed numbers, besides the OS mass scheme, we compute the Higgs p_T distribution using for the first time a dynamical mass renormalisation scheme, the $\overline{\text{MS}}$ scheme.

2. Calculation

Our computation of the Higgs p_T distribution is based on amplitudes which are valid for arbitrary quark masses circulating in the heavy-quark loops.

We consider the production of a Higgs boson in association with a jet in proton-proton collisions, $p + p \to H + j + X$. The corresponding cross section can be found by convoluting the partonic cross section with the respective parton distribution functions (PDF), for the partonic channels: $gg \to Hg$, $q\bar{q} \to Hg$ and $q(\bar{q})g \to Hq(\bar{q})$. At LO in the coupling constants, this involves the one-loop $2 \to 2$ amplitudes. The coupling of the Higgs boson to light quarks is suppressed by the light-quark mass. Therefore, only the contributions in which the Higgs boson is coupled to a heavy quark are important. In this letter we consider the contribution of the top and the bottom quarks.

At NLO in QCD, we have to consider the $\mathcal{O}(\alpha_S)$ corrections to the LO $2 \to 2$ amplitudes, together with the one-loop $2 \to 3$ amplitudes, in which the Higgs boson and the jet are produced with an additional parton in the final state: $gg \to Hgg$, $q\bar{q} \to Hgg$, and $q(\bar{q})g \to Hq(\bar{q})g$. The calculation of the two-loop $2 \to 2$ amplitudes, which has been performed assembling the relevant master integrals [48–50], is briefly described in the following subsection and will be the subject of a forthcoming publication [51]. The calculation of the one-loop $2 \to 3$ amplitudes, which are known analytically [52,53] and numerically through public automated tools, has been performed using the results of refs. [53,54] reported in the program MCFM-9.1 [55]. We have cross-checked the one-loop $2 \to 3$ amplitudes with automated tools (MG5_aMC@NLO [34,56] and GoSam [57]) and found perfect agreement for every phase-space point we compared, including points where an unresolved limit is approached.

After renormalisation of the ultra-violet (UV) divergences, each of the two sets of amplitudes still contains infra-red (IR) divergences. In order to regulate such divergences, we used the dipole subtraction scheme [58]. For the numerical evaluation of the $2 \to 3$ amplitudes and the subtraction terms, both local and integrated, we have used the program MCFM-9.1 [55]. Although the integration of the $2 \to 3$ amplitudes, even when generated with the automated tools, is not time intensive, we preferred to use the analytic result of refs. [53,54] which saved about a factor of a hundred in the integration time of the gluonic one-loop $2 \to 3$ amplitudes.

3. Two-loop $2 \to 2$ amplitudes

The two-loop $2 \to 2$ amplitudes for the processes under consideration can be written in terms of form factors, exploiting their Lorentz and Dirac structures, where every form factor can be expressed as a combination of scalar integrals that are divergent in four space-time dimensions. We regularise both UV and IR divergences in dimensional regularisation. Since the scalar integrals are not all independent, we use Integration-by-Parts Identities [59–61], implemented in the computer programs FIRE [62,63] and Kira [64,65], in order to reduce them to a set of independent integrals, called Master Integrals (MIs). We calculate the MIs using the differential equations method [66–73]. The MIs are expressed as Laurent series in the dimensional parameter $\epsilon = (4 - d)/2$, where d is the dimension of space-time. The system of first-order linear differential equations satisfied by the MIs is solved at every order in ϵ using DiffExp [74], a Mathematica implementation of the series-expansion method [75]. The evaluation of all the 447 MIs involved in the calculation is described in detail in [48–50]. For a number of points in the physical phase space region we compared the values of the full set of MIs with results obtained using the numerical package AMFlow [76,77], always finding agreement with the requested full precision (16 digits).

The bare two-loop $2 \to 2$ amplitudes need UV renormalisation. To establish the impact of the choice of renormalization schemes and the contribution of top-bottom interference we have considered three different calculations. In the first two, the bottom is the fifth massless quark and only the top quark is massive. We employ two different schemes that differ only in the renormalization of the heavy quark mass. In particular, we renormalise the external fields on-shell and the strong coupling constant in a mixed scheme in which the light-flavour contribution is renormalised in $\overline{\text{MS}}$ while the top quark is renormalised at zero momentum. In the first scheme the top quark Yukawa coupling and mass are renormalised OS. In the second scheme, we renormalise both the top quark Yukawa coupling and mass in $\overline{\text{MS}}$. In the third computation we also include the effect of having an internal massive bottom quark attached to the Higgs boson. For a consistent use of the decoupling scheme with five-flavour evolution of the strong coupling and PDFs we have chosen to retain the bottom mass only in the loop where it is coupled to the Higgs boson and set it to zero in the other pure QCD fermion loop. For this third computation we have renormalised both the Yukawa couplings and heavy quark masses in $\overline{\text{MS}}$.

Once the UV divergences are renormalised, the two-loop $2 \to 2$ amplitudes still contain residual IR divergences that appear as poles in $1/\epsilon$. The structure of these IR poles is universal and is described by factorization formulae [58].

We examined the behaviour of the two-loop $2 \to 2$ amplitudes in the soft and collinear limits of one unresolved parton. To do so, we generated sequences of phase space points tending to the desired limit and compared the value of the amplitudes to that predicted by the corresponding one-loop IR factorization formulae [78–83]. We found that the amplitudes approach the limit formulae with the rate expected from the cancellation of the leading singularity order-by-order in ϵ. We observed the expected behaviour of the full amplitudes independently of the value of internal quark mass as well as for the interference of two massive internal quarks.

As a further check, we verified that in the limit of very large transverse momentum, the full amplitude is in reasonable agreement with the approximated results computed in ref. [84].

4. The cross section

The results for the hadronic cross sections have been obtained by combining the integration of the one-loop $2 \to 2$ (Born) and $2 \to 3$ (real) amplitudes, including the subtractions and the initial-state collinear remnants, with the integration of the two-loop $2 \to 2$ (virtual) amplitudes. To efficiently integrate the virtual part we have first produced a grid using the virtual correction in the HEFT. To increase the precision in the computation of the tail of the Higgs p_t distribution, we have biased the weight with an appropriate exponential factor and generated a second grid. Subsequently we have used these grids to integrate the amplitudes in the full theory. In particular for every choice of scales we have run

about 14k points on the cross section grid and 16k on the biased one. When we use the $\overline{\text{MS}}$ mass renormalisation, the value of the internal quark masses changes dynamically in each phase space point so that no form factors or integrals can be recycled from the evaluation of another point. The run time of the evaluation of the two-loop matrix element for one kinematic configuration and one choice of masses circulating in the loops varies greatly depending on the phase-space point and the existing pre-computed points that DiffExp can transport from. However, we can qualitatively report that it ranges from 5 minutes to one hour, with a median around 15 minutes.

We implemented our two-loop amplitudes through a MadGraph5_aMC@NLO plugin, similar to what was done in ref. [43], where the amplitude appeared as an effective vertex in a UFO [85] model. In that representation, the form factors are understood as dynamical couplings which will be re-evaluated for each phase-space point by the tree-level Fortran matrix element code via an interface to Mathematica. The main advantage of such an implementation is that it greatly facilitates the distribution and reproducibility of our two-loop amplitude as it can now readily be generated like any tree-level process in a version of MadGraph5_aMC@NLO equipped with our plugin. It moreover offers additional flexibility regarding the selection of the type of contribution the user is interested in. This includes 1) the possibility of choosing between OS and $\overline{\text{MS}}$ mass renormalisation schemes, 2) selecting particular interference terms and which massive quark flavours are included in each fermion loop, 3) potentially attaching Higgs decay structures to the production process and finally 4) computing renormalisation scale variations through a reweighting procedure necessitating only a single evaluation of the form factors.

For the case of OS top-quark mass renormalisation, we validated this implementation by aligning our setup with that chosen in refs. [35,36] and found adequate agreement both at the inclusive and differential level.[1]

5. Results

In this section we show a selection of predictions obtained using our computation. For our simulation we use the value $G_F = 1.16639 \cdot 10^{-5}$ GeV^{-2} for the Fermi constant and the NNPDF40_nlo_as_01180 [86] PDFs set and α_S. Jets are reconstructed using the anti-kt algorithm [87] with resolution variable $R = 0.4$. We select events of proton-proton collisions at $\sqrt{s} = 13$ TeV where the Higgs boson is produced in association with a jet with transverse momentum larger than $p_T^{j_1} > 20$ GeV. The masses of the Higgs boson and of the internal quarks are set to $m_H = 125.25$ GeV, and $m_t^{\text{OS}} = 172.5$ GeV when considering on-shell top mass renormalisation, whereas we compute $m_t^{\overline{\text{MS}}}(\mu_R)$ from $m_t^{\overline{\text{MS}}}(m_t^{\overline{\text{MS}}}) = 163.4$ GeV in the case of $\overline{\text{MS}}$ top-quark mass renormalisation, using leading logarithmic evolution. The bottom-quark mass and the corresponding Yukawa coupling are computed evolving $m_b^{\overline{\text{MS}}}(\mu_R)$ from $m_b^{\overline{\text{MS}}}(m_b^{\overline{\text{MS}}}) = 4.18$ GeV (also with leading logarithmic accuracy). Our choice for the central renormalisation (μ_R) and factorization (μ_F) scales is

$$\mu_R^0 = \mu_F^0 = \frac{H_T}{2} = \frac{1}{2}\left(\sqrt{m_H^2 + p_{t,H}^2} + \sum_i |p_{t,i}|\right), \tag{1}$$

with the sum running over all partons in the final state. As for the scale variations, we take the envelope of the seven scale choices obtained by varying the central scales by a factor of two in both directions excluding the maximal distance.

Table 1
Cross section for Higgs boson production in association with a jet with transverse momentum larger than $p_T^{j_1} > 20$ GeV, with top- and bottom-quarks circulating in the heavy-quark loop, in the $\overline{\text{MS}}$ scheme (upper line); with top-quark circulating in the loop, in the $\overline{\text{MS}}$ scheme (middle line) and in the OS scheme (lower line), at LO and NLO accuracy.

renormalisation of internal masses	σ_{LO} [pb]	σ_{NLO} [pb]
top+bottom–($\overline{\text{MS}}$)	$12.318^{+4.711}_{-3.117}$	$19.89(8)^{+2.84}_{-3.19}$
top–($\overline{\text{MS}}$)	$12.538^{+4.822}_{-3.183}$	$19.90(8)^{+2.66}_{-2.85}$
top–(OS)	$12.551^{+4.933}_{-3.244}$	$20.22(8)^{+3.06}_{-3.09}$

Our results for the semi-inclusive Higgs production cross section within our jet acceptance cut are given in Table 1, where we note that the relative scale uncertainty goes down from about 30% at LO to about 14% at NLO. Further, by comparing the first two lines, we see that the top-bottom interference yields a negative contribution at LO, and instead a positive contribution at NLO which cancels the offset between the cross section with and without top-bottom interference.

The bottom quark is expected to affect the production rate only at small and intermediate values of the Higgs p_T distribution. Approximated results for the effect of the bottom quark at intermediate p_T values have been previously reported in [41]. In Fig. 1, we show the results of our exact computation for the Higgs p_T distribution in 20 GeV-wide bins at intermediate p_T values, at LO (left panel) and NLO (right panel) accuracy, with top- and bottom-quarks circulating in the heavy-quark loops in $\overline{\text{MS}}$ (black curve); with top-quark only, in $\overline{\text{MS}}$ (blue curve) and in OS (red curve). Vertical bars represent the statistical error from the Monte Carlo integration. In the left panel, the first bin is empty, since the LO kinematic constraint, $p_T = p_T^j$, forces the Higgs p_T to be not lower than 20 GeV; in the second bin, the contribution of the top-bottom interference is negative, and fades away from the third on. In the right panel, the NLO contribution of the top-bottom interference is negative in the first bin, positive in the second, negative again, but smaller, in the third, and dies out from the fourth on. Note that the seven-point scale variation (not shown) provides a much larger uncertainty than the difference among the bars that are shown in the figure. Also note that at LO, the impact of the change of top-quark mass renormalisation scheme is almost indiscernible in the second bin of the left panel. However, at NLO this impact is far greater, and overall 15 times larger than at LO in our semi-inclusive cross-section of Table 1. We leave further investigation of this enhanced sensitivity to the mass and Yukawa renormalisation scheme at NLO to future work.

While the scale uncertainty is expected to be reduced in a resumed calculation of the Higgs p_T, we anticipate that the difference among the different predictions will persist. Further investigation of the Higgs p_T distribution in the low-energy limit is beyond the aim of the present work and will be presented elsewhere.

In Fig. 2, we plot the Higgs p_T distribution in 25 GeV-wide bins, with top- and bottom-quarks circulating in the heavy-quark loops in $\overline{\text{MS}}$, at LO (green curve) and NLO (red curve) accuracy. The scale uncertainty bands at LO (yellow band) and NLO (purple band) accuracy are obtained by taking the envelope of seven-point scale variations. Not to clutter the plot, we refrain from showing the same distribution with the top-quark only, either in $\overline{\text{MS}}$ or in OS, opting for highlighting their behaviour in the next figures. In Fig. 3, we plot the ratio of the Higgs p_T distribution at NLO over the same at LO in 50 GeV-wide bins, with top- and bottom-quarks circulating in the heavy-quark loops, in $\overline{\text{MS}}$ (upper panel); with top-quark

[1] Note that in the erratum version of ref. [35] and in ref. [36], a bug fix is reported that affected the results of ref. [35] by about 13% on the total cross section. We find agreement with the erratum version of ref. [35] and with ref. [36].

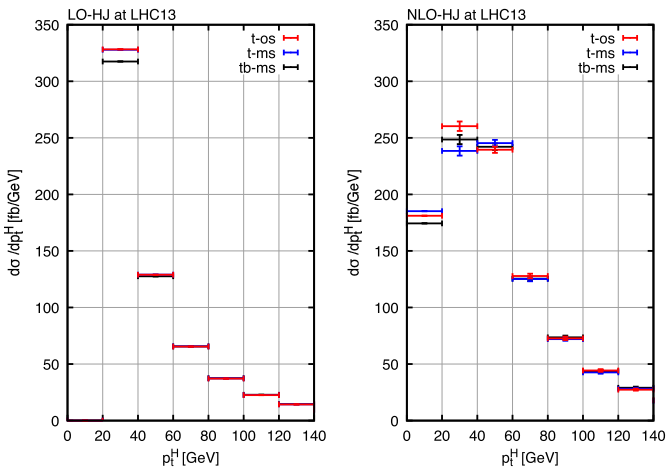

Fig. 1. Higgs p_T distribution in the intermediate p_T range.

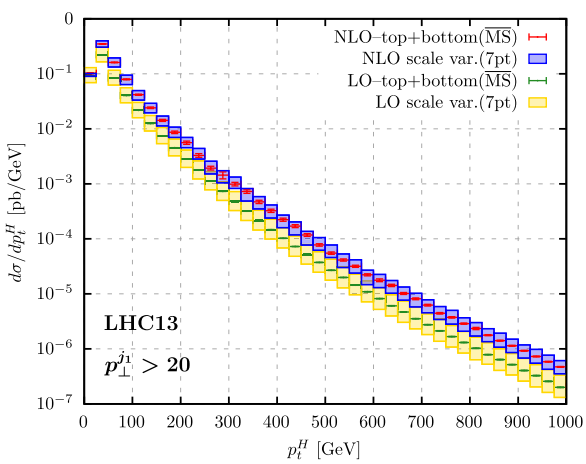

Fig. 2. Higgs p_T distribution with top- and bottom-quarks.

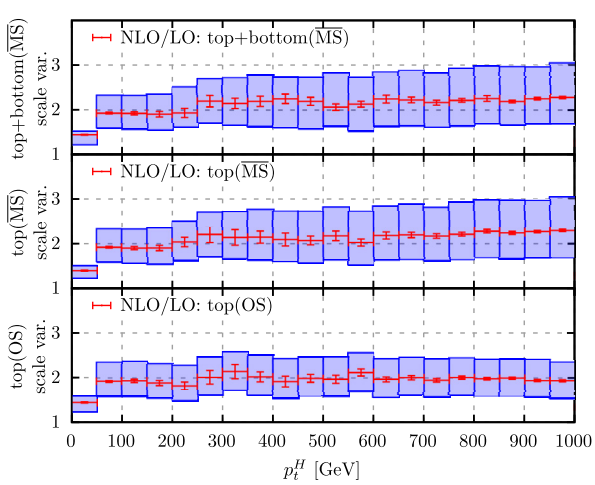

Fig. 3. NLO/LO ratio of the Higgs p_T distribution.

only, in $\overline{\text{MS}}$ (middle panel) and in OS (lower panel). The scale uncertainty bands are given by the ratio of the bands at NLO accuracy over the central value of the Higgs p_T distribution at LO. The upper panel corresponds to the ratio of the red and green curves of Fig. 2. We note that except for the first bin all ratios have a numerical value greater than or equal 2. In particular, the curves of the upper and middle panels have a similar, rather flat, shape with a numerical value which is larger than 2 on most of the p_T

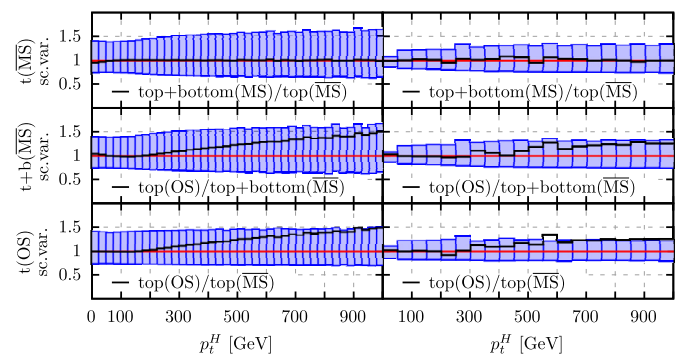

Fig. 4. Ratio of Higgs p_T distributions at LO (left) and NLO (right).

range, while the curve of the lower panel lies near the value 2. In Fig. 4, we plot the ratio of the Higgs p_T distribution, with top- and bottom-quarks circulating in the heavy-quark loops, over the distribution with the top-quark only, both in $\overline{\text{MS}}$ (upper panel); the ratio of the distribution with the top-quark in OS over the one with top- and bottom-quarks in $\overline{\text{MS}}$ (middle panel); the ratio of the distribution with the top-quark in OS over the one with the top-quark in $\overline{\text{MS}}$ (lower panel). The scale uncertainty bands as reported in the y-labels are given by the ratio of the bands of the distributions over their central values. In the left panel of Fig. 4 the distributions display 25 GeV-wide bins and have LO accuracy; in the right panel they display 50 GeV-wide bins and have NLO accuracy. Except for the very first bins, the ratio of the Higgs p_T distribution, with top- and bottom-quarks, over the distribution with top-quark only is flat and equals 1 (upper panels of Fig. 4). This emphasises that within the scale uncertainty the contribution of the bottom quark, and thus of the top-bottom interference, to the Higgs p_T distribution is negligible, except at the low end of the p_T range.

Since the central values of the ratios of the upper panels of Fig. 4 equal 1 over almost the whole p_T range, the ratios of the middle and lower panels are basically equal. Focusing on e.g. the lower panels of Fig. 4, we note that the Higgs p_T distribution with the top-quark only in $\overline{\text{MS}}$ falls off faster than the same distribution in OS, as p_T increases, the more so at LO than at NLO accuracy.

In fact, in the kinematical regime where the Higgs boson has large transverse momentum ($p_{t,H}$) the renormalization scale (μ_R) in Eq. (1) increases with $p_{t,H}$ and so $m_t^{\overline{\text{MS}}}(\mu_R)$ decreases. This is also at the origin of the difference between the upper/middle and the lower panels of Fig. 3 at high p_T values.

6. Conclusions

Building on two-loop amplitudes for Higgs + three partons [51], which are valid for arbitrary quark masses circulating in the heavy-quark loops, we have computed for the first time the NLO QCD corrections to the Higgs p_T distribution in Higgs + jet production via gluon fusion, with top and bottom quarks circulating in the heavy-quark loops. The exact mass dependence on the top and bottom quarks has been included using, for the first time in this context, a running mass renormalisation scheme, the $\overline{\text{MS}}$ scheme. We have also provided predictions for the Higgs p_T distribution with only the top quark, in $\overline{\text{MS}}$ and OS schemes.

We find that within the scale uncertainty the LO contribution of the bottom quark, and thus of the top-bottom interference, to the Higgs boson production is almost erased at inclusive level by the NLO corrections. On the other hand, at the low end of the p_T distribution, the interference induces a non trivial change of shape. For precision studies on the high energy tail and with the current attainable accuracy, the use of the Higgs p_T distribution with only the top quark circulating in the heavy-quark loops is

fully justified. Finally, we find that the Higgs p_T distribution with the top-quark only in $\overline{\text{MS}}$ falls off faster than the same distribution in the OS scheme as p_T increases. This would have an obvious impact on any numerical study, requiring then that the choice of mass renormalisation scheme be done with great care.

Declaration of competing interest

The authors declare that they have no known competing financial interests or personal relationships that could have appeared to influence the work reported in this paper.

Data availability

No data was used for the research described in the article.

Acknowledgements

We thank S. Catani, G. Luisoni, F. Maltoni and P. Nason for interesting discussions and A. Schweitzer for his contribution in the earlier development of the interface of multi-loop amplitudes with MadGraph5_aMC@NLO. H.F. has received funding from the European Union's Horizon 2020 research and innovation program under the Marie Skłodowska-Curie grant agreement No. 847523 'INTERACTIONS', and has been partially supported by a Carlsberg Foundation Reintegration Fellowship. M.H. is supported by the European Research Council under ERC-STG-804286 UNISCAMP. R.B. is partly supported by the Italian Ministero della Università e della Ricerca (MIUR) under grant PRIN 20172LNEEZ. G.S. was supported by grant K 143451 of the National Research, Development and Innovation Fund in Hungary and by the Bolyai Fellowship programme of the Hungarian Academy of Sciences.

References

[1] G. Aad, et al., ATLAS, Phys. Lett. B 716 (2012) 1, arXiv:1207.7214 [hep-ex].
[2] S. Chatrchyan, et al., CMS, Phys. Lett. B 716 (2012) 30, arXiv:1207.7235 [hep-ex].
[3] C. Arnesen, I.Z. Rothstein, J. Zupan, Phys. Rev. Lett. 103 (2009) 151801, arXiv:0809.1429 [hep-ph].
[4] R.V. Harlander, T. Neumann, Phys. Rev. D 88 (2013) 074015, arXiv:1308.2225 [hep-ph].
[5] A. Banfi, A. Martin, V. Sanz, J. High Energy Phys. 08 (2014) 053, arXiv:1308.4771 [hep-ph].
[6] A. Azatov, A. Paul, J. High Energy Phys. 01 (2014) 014, arXiv:1309.5273 [hep-ph].
[7] C. Grojean, E. Salvioni, M. Schlaffer, A. Weiler, J. High Energy Phys. 05 (2014) 022, arXiv:1312.3317 [hep-ph].
[8] M. Schlaffer, M. Spannowsky, M. Takeuchi, A. Weiler, C. Wymant, Eur. Phys. J. C 74 (2014) 3120, arXiv:1405.4295 [hep-ph].
[9] M. Buschmann, C. Englert, D. Goncalves, T. Plehn, M. Spannowsky, Phys. Rev. D 90 (2014) 013010, arXiv:1405.7651 [hep-ph].
[10] S. Dawson, I.M. Lewis, M. Zeng, Phys. Rev. D 90 (2014) 093007, arXiv:1409.6299 [hep-ph].
[11] M. Buschmann, D. Goncalves, S. Kuttimalai, M. Schonherr, F. Krauss, T. Plehn, J. High Energy Phys. 02 (2015) 038, arXiv:1410.5806 [hep-ph].
[12] D. Ghosh, M. Wiebusch, Phys. Rev. D 91 (2015) 031701, arXiv:1411.2029 [hep-ph].
[13] S. Dawson, I.M. Lewis, M. Zeng, Phys. Rev. D 91 (2015) 074012, arXiv:1501.04103 [hep-ph].
[14] U. Langenegger, M. Spira, I. Strebel, arXiv:1507.01373 [hep-ph], 2015.
[15] A. Azatov, C. Grojean, A. Paul, E. Salvioni, J. High Energy Phys. 09 (2016) 123, arXiv:1608.00977 [hep-ph].
[16] M. Grazzini, A. Ilnicka, M. Spira, M. Wiesemann, J. High Energy Phys. 03 (2017) 115, arXiv:1612.00283 [hep-ph].
[17] N. Deutschmann, C. Duhr, F. Maltoni, E. Vryonidou, J. High Energy Phys. 12 (2017) 063, Erratum: J. High Energy Phys. 02 (2018) 159, arXiv:1708.00460 [hep-ph].
[18] A. Banfi, B.M. Dillon, W. Ketaiam, S. Kvedaraite, J. High Energy Phys. 01 (2020) 089, arXiv:1905.12747 [hep-ph].
[19] M. Battaglia, M. Grazzini, M. Spira, M. Wiesemann, J. High Energy Phys. 11 (2021) 173, arXiv:2109.02987 [hep-ph].
[20] H. Georgi, S. Glashow, M. Machacek, D.V. Nanopoulos, Phys. Rev. Lett. 40 (1978) 692.
[21] D. Graudenz, M. Spira, P.M. Zerwas, Phys. Rev. Lett. 70 (1993) 1372.
[22] M. Spira, A. Djouadi, D. Graudenz, P.M. Zerwas, Nucl. Phys. B 453 (1995) 17, arXiv:hep-ph/9504378 [hep-ph].
[23] M. Czakon, R.V. Harlander, J. Klappert, M. Niggetiedt, Phys. Rev. Lett. 127 (2021) 162002, arXiv:2105.04436 [hep-ph].
[24] R.V. Harlander, W.B. Kilgore, Phys. Rev. Lett. 88 (2002) 201801, arXiv:hep-ph/0201206 [hep-ph].
[25] C. Anastasiou, K. Melnikov, Nucl. Phys. B 646 (2002) 220, arXiv:hep-ph/0207004 [hep-ph].
[26] V. Ravindran, J. Smith, W.L. van Neerven, Nucl. Phys. B 665 (2003) 325, arXiv:hep-ph/0302135 [hep-ph].
[27] V. Khachatryan, et al., CMS, J. High Energy Phys. 03 (2017) 032, arXiv:1606.01522 [hep-ex].
[28] A.M. Sirunyan, et al., CMS, Phys. Rev. Lett. 120 (2018) 071802, arXiv:1709.05543 [hep-ex].
[29] G. Aad, et al., ATLAS, Eur. Phys. J. C 79 (2019) 836, arXiv:1906.11005 [hep-ex].
[30] A.M. Sirunyan, et al., CMS, J. High Energy Phys. 12 (2020) 085, arXiv:2006.13251 [hep-ex].
[31] K. Becker, et al., arXiv:2005.07762 [hep-ph], 2020.
[32] R.K. Ellis, I. Hinchliffe, M. Soldate, J.J. van der Bij, Nucl. Phys. B 297 (1988) 221.
[33] U. Baur, E.W.N. Glover, Nucl. Phys. B 339 (1990) 38.
[34] V. Hirschi, O. Mattelaer, J. High Energy Phys. 10 (2015) 146, arXiv:1507.00020 [hep-ph].
[35] S.P. Jones, M. Kerner, G. Luisoni, Phys. Rev. Lett. 120 (2018) 162001, Erratum: Phys. Rev. Lett. 128 (2022) 059901, arXiv:1802.00349 [hep-ph].
[36] X. Chen, A. Huss, S.P. Jones, M. Kerner, J.N. Lang, J.M. Lindert, H. Zhang, J. High Energy Phys. 03 (2022) 096, arXiv:2110.06953 [hep-ph].
[37] J.M. Lindert, K. Kudashkin, K. Melnikov, C. Wever, Phys. Lett. B 782 (2018) 210, arXiv:1801.08226 [hep-ph].
[38] K. Melnikov, A. Penin, J. High Energy Phys. 05 (2016) 172, arXiv:1602.09020 [hep-ph].
[39] E. Braaten, H. Zhang, J.-W. Zhang, Phys. Rev. D 97 (2018) 096014, arXiv:1707.09857 [hep-ph].
[40] F. Caola, J.M. Lindert, K. Melnikov, P.F. Monni, L. Tancredi, C. Wever, J. High Energy Phys. 09 (2018) 035, arXiv:1804.07632 [hep-ph].
[41] J.M. Lindert, K. Melnikov, L. Tancredi, C. Wever, Phys. Rev. Lett. 118 (2017) 252002, arXiv:1703.03886 [hep-ph].
[42] F. Caola, S. Forte, S. Marzani, C. Muselli, G. Vita, J. High Energy Phys. 08 (2016) 150, arXiv:1606.04100 [hep-ph].
[43] M. Becchetti, R. Bonciani, V. Del Duca, V. Hirschi, F. Moriello, A. Schweitzer, Phys. Rev. D 103 (2021) 054037, arXiv:2010.09451 [hep-ph].
[44] R. Boughezal, F. Caola, K. Melnikov, F. Petriello, M. Schulze, J. High Energy Phys. 06 (2013) 072, arXiv:1302.6216 [hep-ph].
[45] X. Chen, T. Gehrmann, E.W.N. Glover, M. Jaquier, Phys. Lett. B 740 (2015) 147, arXiv:1408.5325 [hep-ph].
[46] R. Boughezal, F. Caola, K. Melnikov, F. Petriello, M. Schulze, Phys. Rev. Lett. 115 (2015) 082003, arXiv:1504.07922 [hep-ph].
[47] R. Boughezal, C. Focke, W. Giele, X. Liu, F. Petriello, Phys. Lett. B 748 (2015) 5, arXiv:1505.03893 [hep-ph].
[48] R. Bonciani, V. Del Duca, H. Frellesvig, J.M. Henn, F. Moriello, V.A. Smirnov, J. High Energy Phys. 12 (2016) 096, arXiv:1609.06685 [hep-ph].
[49] R. Bonciani, V. Del Duca, H. Frellesvig, J.M. Henn, M. Hidding, L. Maestri, F. Moriello, G. Salvatori, V.A. Smirnov, J. High Energy Phys. 01 (2020) 132, arXiv:1907.13156 [hep-ph].
[50] H. Frellesvig, M. Hidding, L. Maestri, F. Moriello, G. Salvatori, J. High Energy Phys. 06 (2020) 093, arXiv:1911.06308 [hep-ph].
[51] R. Bonciani, V. Del Duca, H. Frellesvig, M. Hidding, V. Hirschi, F. Moriello, G. Salvatori, G. Somogyi, F. Tramontano, in preparation.
[52] V. Del Duca, W. Kilgore, C. Oleari, C. Schmidt, D. Zeppenfeld, Nucl. Phys. B 616 (2001) 367, arXiv:hep-ph/0108030.
[53] L. Budge, J.M. Campbell, G. De Laurentis, R.K. Ellis, S. Seth, J. High Energy Phys. 05 (2020) 079, arXiv:2002.04018 [hep-ph].
[54] R.K. Ellis, S. Seth, J. High Energy Phys. 11 (2018) 006, arXiv:1808.09292 [hep-ph].
[55] J. Campbell, T. Neumann, J. High Energy Phys. 12 (2019) 034, arXiv:1909.09117 [hep-ph].
[56] J. Alwall, R. Frederix, S. Frixione, V. Hirschi, F. Maltoni, O. Mattelaer, H.S. Shao, T. Stelzer, P. Torrielli, M. Zaro, J. High Energy Phys. 07 (2014) 079, arXiv:1405.0301 [hep-ph].
[57] G. Cullen, et al., Eur. Phys. J. C 74 (2014) 3001, arXiv:1404.7096 [hep-ph].
[58] S. Catani, M.H. Seymour, Nucl. Phys. B 485 (1997) 291, Erratum: Nucl. Phys. B 510 (1998) 503–504, arXiv:hep-ph/9605323.
[59] F.V. Tkachov, Phys. Lett. B 100 (1981) 65.
[60] K.G. Chetyrkin, F.V. Tkachov, Nucl. Phys. B 192 (1981) 159.
[61] S. Laporta, Int. J. Mod. Phys. A 15 (2000) 5087, arXiv:hep-ph/0102033.
[62] A.V. Smirnov, J. High Energy Phys. 10 (2008) 107, arXiv:0807.3243 [hep-ph].
[63] A.V. Smirnov, F.S. Chuharev, Comput. Phys. Commun. 247 (2020) 106877, arXiv:1901.07808 [hep-ph].

[64] P. Maierhöfer, J. Usovitsch, P. Uwer, Comput. Phys. Commun. 230 (2018) 99, arXiv:1705.05610 [hep-ph].
[65] J. Klappert, F. Lange, P. Maierhöfer, J. Usovitsch, Comput. Phys. Commun. 266 (2021) 108024, arXiv:2008.06494 [hep-ph].
[66] A.V. Kotikov, Phys. Lett. B 254 (1991) 158.
[67] A.V. Kotikov, Phys. Lett. B 267 (1991) 123, Erratum: Phys. Lett. B 295 (1992) 409.
[68] Z. Bern, L.J. Dixon, D.A. Kosower, Nucl. Phys. B 412 (1994) 751, arXiv:hep-ph/9306240.
[69] E. Remiddi, Nuovo Cimento A 110 (1997) 1435, arXiv:hep-th/9711188 [hep-th].
[70] T. Gehrmann, E. Remiddi, Nucl. Phys. B 580 (2000) 485, arXiv:hep-ph/9912329 [hep-ph].
[71] M. Argeri, P. Mastrolia, Int. J. Mod. Phys. A 22 (2007) 4375, arXiv:0707.4037 [hep-ph].
[72] J.M. Henn, Phys. Rev. Lett. 110 (2013) 251601, arXiv:1304.1806 [hep-th].
[73] J.M. Henn, J. Phys. A 48 (2015) 153001, arXiv:1412.2296 [hep-ph].
[74] M. Hidding, Comput. Phys. Commun. 269 (2021) 108125, arXiv:2006.05510 [hep-ph].
[75] F. Moriello, J. High Energy Phys. 01 (2020) 150, arXiv:1907.13234 [hep-ph].
[76] X. Liu, Y.-Q. Ma, C.-Y. Wang, Phys. Lett. B 779 (2018) 353, arXiv:1711.09572 [hep-ph].
[77] X. Liu, Y.-Q. Ma, arXiv:2201.11669 [hep-ph], 2022.
[78] Z. Bern, L.J. Dixon, D.C. Dunbar, D.A. Kosower, Nucl. Phys. B 425 (1994) 217, arXiv:hep-ph/9403226.
[79] Z. Bern, V. Del Duca, C.R. Schmidt, Phys. Lett. B 445 (1998) 168, arXiv:hep-ph/9810409.
[80] D.A. Kosower, Nucl. Phys. B 552 (1999) 319, arXiv:hep-ph/9901201.
[81] D.A. Kosower, P. Uwer, Nucl. Phys. B 563 (1999) 477, arXiv:hep-ph/9903515.
[82] Z. Bern, V. Del Duca, W.B. Kilgore, C.R. Schmidt, Phys. Rev. D 60 (1999) 116001, arXiv:hep-ph/9903516.
[83] S. Catani, M. Grazzini, Nucl. Phys. B 591 (2000) 435, arXiv:hep-ph/0007142.
[84] K. Kudashkin, K. Melnikov, C. Wever, J. High Energy Phys. 02 (2018) 135, arXiv:1712.06549 [hep-ph].
[85] C. Degrande, C. Duhr, B. Fuks, D. Grellscheid, O. Mattelaer, T. Reiter, Comput. Phys. Commun. 183 (2012) 1201, arXiv:1108.2040 [hep-ph].
[86] R.D. Ball, et al., NNPDF, Eur. Phys. J. C 82 (2022) 428, arXiv:2109.02653 [hep-ph].
[87] M. Cacciari, G.P. Salam, G. Soyez, J. High Energy Phys. 04 (2008) 063, arXiv:0802.1189 [hep-ph].